Intramolecular Electron Transfer between Doubly Six σ-Bond-Linked Trialkyldiazenium Cation and Diazenyl Radical Units

Stephen F. Nelsen,* Dwight A. Trieber, II, J. Jens Wolff, Douglas R. Powell, and Shervalen Rogers-Crowley

Contribution from the Department of Chemistry, University of Wisconsin, 1101 University Avenue, Madison, Wisconsin 53706-1396

Received September 30, 1996. Revised Manuscript Received May 4, 1997[⊗]

Abstract: Rate constants k_{ESR} for intramolecular electron transfer between the reduced and oxidized diazene units of dimeric 2-*tert*-butyl-2,3-diazabicyclo[2.2.2]octyldiazenium radical cations cations which are doubly linked through the bicyclic units by six σ-bonds, **sB6**σ^+ and **aB6**σ^+, were determined from their variable temperature ESR spectra in CH_3CN, dimethylformamide, and CH_2Cl_2. These cations show solvent−sensitive charge transfer absorption bands from which the vertical electron transfer excitation energy, λ, and the electronic coupling, V_J, were determined by simulation, using vibronic coupling theory. The partitioning between solvent and vibrational components of λ were made assuming that the average energy of the vibrational modes coupled to the electron transfer, $h\nu_v$, is 3.15 kcal/mol (1100 cm^{-1}). The observed rate constants interpolated to 298 K are factors of 4.7−5.8 larger than those calculated from the electron transfer parameters obtained from vibronic coupling theory analysis of the charge transfer bands, k_{cal}, in acetonitrile and DMF, and for **sB6**σ^+ in CH_2Cl_2 the factor is 2.5. The ratios $k_{ESR}(350)/k_{ESR}(250)$ are 1.0−1.6 times larger than $k_{cal}(350)/k_{cal}(250)$in CH_3CN and DMF and 0.9 times larger in CH_2Cl_2. The agreement with theory for the bis-diazeniums is far better than that obtained for doubly four σ-bond-linked bis-hydrazine radical cations (*J. Am. Chem. Soc.* **1997**, *119*, XXXX). It is suggested that the significantly smaller vibronic coupling constants $S = \lambda_v/h\nu_v$ for the bis-diazeniums (6.5−7.6) compared to those of the bis-hydrazines (13.6−17.5) might be principally responsible for the difference in agreement of theory with experiment.

Introduction

In previous work, we prepared organic analogues of mixed-valence complexes[1] from doubly four σ-bond-linked bis-azo compounds **T** and **H**, which were bis-*tert*-butylated to equal mixtures of *anti*- and *syn*-substituted bis-diazenium dication salts.[2] One electron reduction of the *anti* di-*tert*-butyl dication,

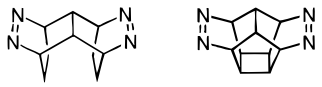

T **H**

for example, gave the monocation **aBT**$^+$, which showed charge transfer (CT) absorption in the near-infrared, as expected for the localized species shown, with one dinitrogen unit at the diazenium cation oxidation state and the other reduced to the neutral diazenyl oxidation state. All three bis-diazenium

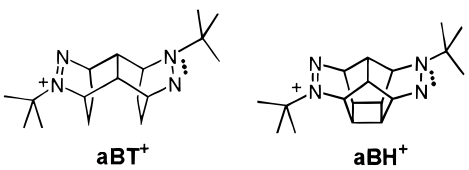

aBT$^+$ **aBH**$^+$

monocations studied (the *syn* diazenium dication from **H** could not be separated from about 15% of the *anti* diastereomer and was not studied) proved to have electron transfer (ET) which was too fast on the ESR time scale to determine rate constants k_{ESR} for intramolecular ET. Although this was qualitatively consistent with prediction from a Marcus−Hush theory analysis of the charge transfer (CT) bands, it precluded the quantitative test of the theory we had hoped to achieve. We have therefore prepared bis-azo compound **6**σ to allow di-*tert*-butylation and reduction to give six σ-bond-linked versions of the bis-diazenium monocations, the *anti* **aB6**σ^+ and its *syn* diastereomer. We hoped that increasing the distance between the

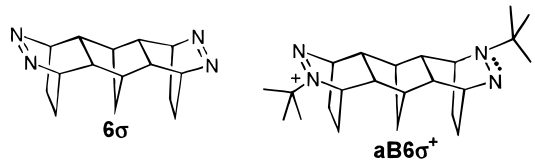

6σ **aB6σ$^+$**

dinitrogen units in going from four to six σ-bond-linking units would lower k_{ESR} enough to bring it into the rate constant window for which the dynamic ESR spectrum is sensitive to exchange rate constant, k_{ESR} near 10^8 s^{-1} for the ca. 11 G nitrogen splittings of trialkylhydrazyls. This proved to be the case.

Results

Bis-azo compound **6**σ was prepared by annealing diazabicyclooctyl units onto norbornadiene using the double tetrachlorocyclopentadieneone acetal Diels−Alder addition, reduction, hydrolysis/decarbonylation, MTAD (**7**) addition route shown in Scheme 1.[3] Although it requires several steps, this route gives only the *out*,*out* azo diastereomer indicated, making it quite efficient. The starting materials are cheap, and **6**σ is far more easily available than **T** and **H**. Compound **6**σ crystallizes in

[⊗] Abstract published in *Advance ACS Abstracts*, July 1, 1997.

(1) For a review of mixed-valence complexes, see: Creutz, C. *Prog. Inorg. Chem.* **1983**, *30*, 1.

(2) (a) Nelsen, S. F.; Chang, H.; Wolff, J. J.; Adamus, J. *J. Am. Chem. Soc.* **1993**, *115*, 12276. (b) Nelsen, S. F.; Chang, H.; Powell, D. R. *J. Org. Chem.* **1994**, *59*, 6558.

S0002-7863(96)03417-8 CCC: $14.00

Scheme 1

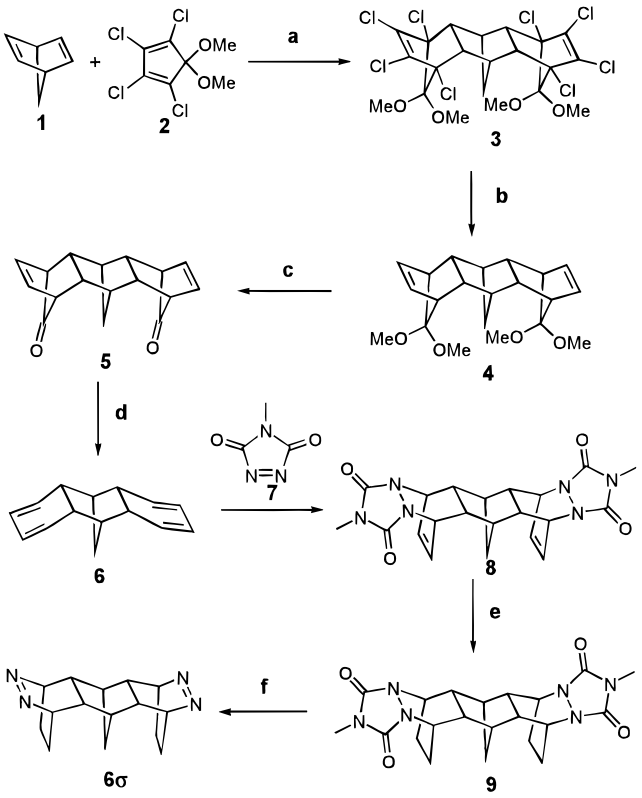

[a] Key: a. reflux, C_6H_5Cl; b. Na, tBuOH, THF; c. $HClO_4$, THF; d. reflux, THF; e. H_2, Pd/C, CH_3CO_2H; f. (1) KOH, iPrOH; (2) HCl, $CuCl_2$; (3) NH_4OH.

Table 1. Comparison of Bis-Azo Compound and Bis-Olefin Photoelectron Spectroscopic Data

compd	vIP$_1$ (eV)[a]	vIP$_2$ (eV)[a]	V_{PE} (kcal/mol)[b]	$\|E\|/2$ (kcal/mol)
T	7.90(A_2)	8.86(B_2)	11.1	7.9(5.0)
H	8.14(A_2)	8.85(B_2)	8.1	5.8(3.5)
6σ	7.86(A_2)	8.20(B_2)	3.9	3.3(1.3)
10(4σ**)**[d]	8.48(B_1)	9.35(A_1)	10.0	6.3(3.9)
10(6σ**)**[d]	8.58(B_1)	8.90(A_1)	3.7	1.8(1.0)

[a] SOMO symmetry in C_{2v} molecular symmetry is shown in parentheses. [b] $V_{PE} = \Delta vIP/2$; see ref 4 and the Discussion section. [c] Calculated V_{PE} estimated as half of the difference in eigenvalues, E, for the HOMO and (HOMO-1) of the neutral compound, which in each case corresponds to the assignment given. The result from an AM1 calculation is followed (in parentheses) by that for a PM3 calculation. [d] From ref 3.

space group C_2/m, with a mirror plane down the long axis of the molecule, bisecting the NN bonds and passing through the methylene bridge of the bicylo[2.2.1]heptyl ring in the center of the molecule, so it is not twisted about the long axis. The perpendicular mirror plane formally expected is not present in the crystal, the NN distances are 1.253(4) and 1.264(4) Å, and the distance between the azo groups across the molecule is 7.184 Å.

The photoelectron (PE) spectra of bis-azo compounds **T**, **H**, and **6**σ have been obtained, and the lone pair vertical ionization potentials (vIP), which are the only bands clearly resolved, are summarized in Table 1. Also included in Table 1 for comparison are literature data for π ionizations of doubly four- and six σ-bond-linked olefins **10(4**σ**)** and **10(6**σ**)**.[4]

(3) This route for stereospecific conversion of a norbornene double bond to a diazabicyclo[2.2.2]octane unit was devised by W. L. Mock (University of Illinois−Chicago), who applied it to a cyclopentadiene trimer (unpublished), and was kind enough to tell us about it and supply experimental details.

Table 2. Cyclic Voltammetry data for *syn*- and *anti*-**B6**σ^{2+} [a]

cmpd	solvent	$E_1^{ox} - E_2^{red}$ (mV)	$E_1°$ (V)	$E_2°$ (V)	$E_2° - E_1°$ (mV)
syn	CH_3CN	180	−0.81	−0.69	120
	DMF	183	−0.73	−0.62	110
	CH_2Cl_2	148	−0.70	-0.60	100
anti	CH_3CN	166	−0.80	-0.68	120
	DMF	156	−0.73	-0.62	110
	CH_2Cl_2	153	−0.71	-0.62	90

[a] Scan rate of 200 mV/s at Pt in solvent containing 0.1 M Bu_4NClO_4 vs SCE. Formal potentials determined by simulation and are not good to better than 0.01 V.

10(4σ) **10(6σ)**

Conveniently, the bis-diazenium cation isomers of **B6**σ^{2+} can be rather cleanly separated simply by filtering the hot solution obtained after refluxing it with $HBF_4 \cdot Et_2O$ in *tert*-butyl alcohol to accomplish the *tert*-butylation. Species **sB6**$\sigma^{2+}(BF_4^-)_2$ is quite insoluble, but almost all of the **aB6**$\sigma^{2+}(BF_4^-)_2$ remains in solution. The *syn* compound has different norbornyl bridgehead carbons and the *anti* does not, making these assignments certain from their ^{13}C NMR spectra. This easy separation was especially appreciated because the separation of the bis-diazenium dications derived from **T** involved a tedious physical separation of crystals, and only the less soluble, *anti* isomer ever was obtained pure for the bis-diazenium dications derived from **H**. A crystal structure of **sB6**$\sigma^{2+}(Ph_4B^-)_2(CH_3CN)$ has been obtained. The acetonitrile is disordered and modeled in two orientations with occupancies of 0.600(5) and 0.400(5), and the cation was also disordered and modeled in two orientations about the long axis having occupancies of 0.884(2) and 0.116(2). The standard deviations for the bond distances of the major orientation are one-fourth those for the minor, and only the major one will be discussed (they are quite similar in structure). The N═N distances are 1.261(2) and 1.260(2) Å, at the upper end of the range observed for BF_4^- salts of other compounds containing the 2-*tert*-butyl-2,3-diazabicyclo[2.2.2]-octyldiazenium cation unit.[2b] The trisubstituted nitrogens are within experimental error of being planar. The distance between the trisubstituted nitrogens is 7.076 Å and that between the disubstituted ones is 7.126 Å, so the average distance between the diazenium units is 7.101 Å, 1% shorter than that between the diazine units of the parent azo compound, **6**σ.

Cyclic voltammetry (CV) gave two badly overlapping reversible one-electron reduction waves for each diastereomer, as summarized in Table 2. The difference in the formal redox potentials is about 0.1 V, significantly smaller than that for the four σ-bond-linked compounds (0.35−0.4 V), as expected because the electrostatic and electronic interaction through six bonds are smaller, and formal potentials were determined by simulation of the CV curves, as in our previous work.[2a] The two diastereomers give CV data that are the same within experimental error. Reduction to the *anti*- and *syn*-**B6**σ^+ radical cations was carried out coulometrically, giving blue-green solutions which are exceptionally sensitive to oxygen and water. The lifetimes are solvent dependent in the order DMF > CH_3CN (AN) > CH_2Cl_2 (MC). We believe that this order may be caused by the relative rates of intermolecular disproportionation, but have not done experiments to establish this.

(4) (a) Paddon-Row, M. N.; Patney, H. K.; Brown, R. S.; Houk, K. N. *J. Am. Chem. Soc.* **1981**, *103*, 5575. (b) Paddon-Row, M. N. *Acc. Chem. Res.* **1982**, *15*, 245.

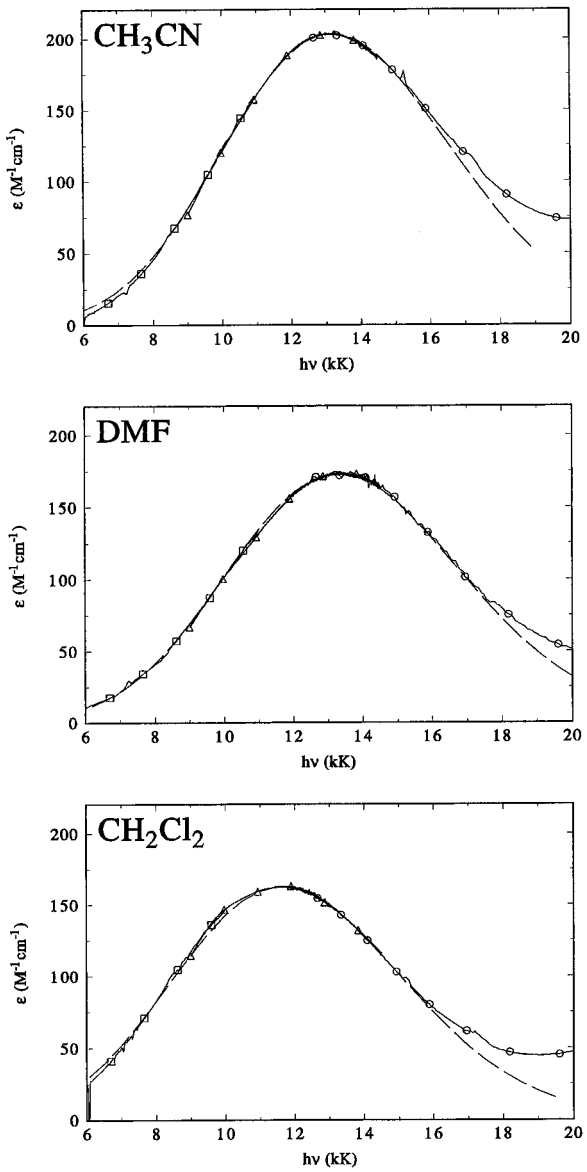

Figure 1. Comparison of the absorption spectra for the CT band region of **sB6**σ^+ in acetonitrile, dimethylformamide, and methylene chloride with calculated spectra using the parameters shown in Table 5. The experimental data (solid lines) are designated with circles (visible spectrometer), triangles (Si detector), and squares (Pb/Se detector) and the calculated spectra are shown as dashed lines.

Solutions of the radical cations show broad CT absorption bands with maxima just beyond the visible region, and to observe the entire band both a visible spectrometer and a near-infrared using both Pb/Se and Si detectors had to be employed. The three data sets were combined by referencing the lowest energy end to zero absorption, which brought the near-infrared Pb/Se detector data set into good registry with the other two sets; agreement of the three regions of the spectrum, which overlap significantly, was good (see Figure 1). Table 3 shows the optical data for both isomers in three solvents at room temperature, along with a Hush analysis.[5]

The **B6**σ^+ ESR spectra are sensitive to both temperature and solvent. The spectrum has the 1:2:3:2:1 five line a(2N) pattern expected for slow ET at low temperature, because the difference between the two a(N) values is not resolved. After passing through a region showing an alternating line width effect, it approaches the nine-line a(4N) pattern expected for ET being fast on the ESR time scale at high temperature. Additional ill-resolved splittings for some of the protons are also observed. The splitting constants for the "frozen" radical are required to carry out simulations to determine k_{et} from the ESR spectra. The "monomeric" hydrazyl radical **11** shows an ESR spectrum with poor resolution which was fit using a(N) = 11.00, a(N) = 10.62, a(2H$_x$) = 2.82, a(2H$_x$′) = 1.82, a(2H) = 0.86, and a(2H) = 0.57, with a line width of 1.4 G.[2a] Each hydrazyl unit of

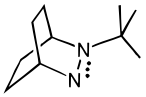

11

aB6σ has one of each of the larger splitting a(2H$_x$) and a(2H$_x$′) hydrogens of **11** removed because of the presence of the linking bridges, and the geometry is also probably slightly different; both the nitrogen splittings and the H$_x$ splittings are probably quite sensitive to geometry. The bis-radical **aB6**σ^0 generated by coulometric reduction in MC shows an ESR spectrum with relatively narrow lines which is simulated using a(N) = 11.7, a(N) = 10.6, a(H) = 3.75, and a(H) = 2.45, with a(4H) = 0.3 and a line width of 1.2 G (see Figure 2). This "bis-radical" spectrum is consistent with that expected for the diazenyl radicals behaving independently, having the dipolar splitting contribution averaged away by thermal tumbling, and provides our best estimate of what the "frozen" spectrum for **B6**σ^+ should be. The ESR spectrum of **aB6**σ^0 in frozen MC at liquid nitrogen temperature shows in addition to a larger narrow line presumably caused by polycrystalline material, triplet features consistent with the dipolar splitting $D' \approx 53.3$ G, which corresponds to d = 8.0$_4$ Å using the point dipole approximation formula, d(Å) = 30.3[D'(G)]$^{-1/3}$.[6] This distance is 12 and 13% larger than the X-ray distance between the dinitrogen units of **6**σ and **sB6**σ^{2+}.

The dynamic ESR fits used the **aB6**σ^0 splittings as a starting point, which were adjusted along with the line width and

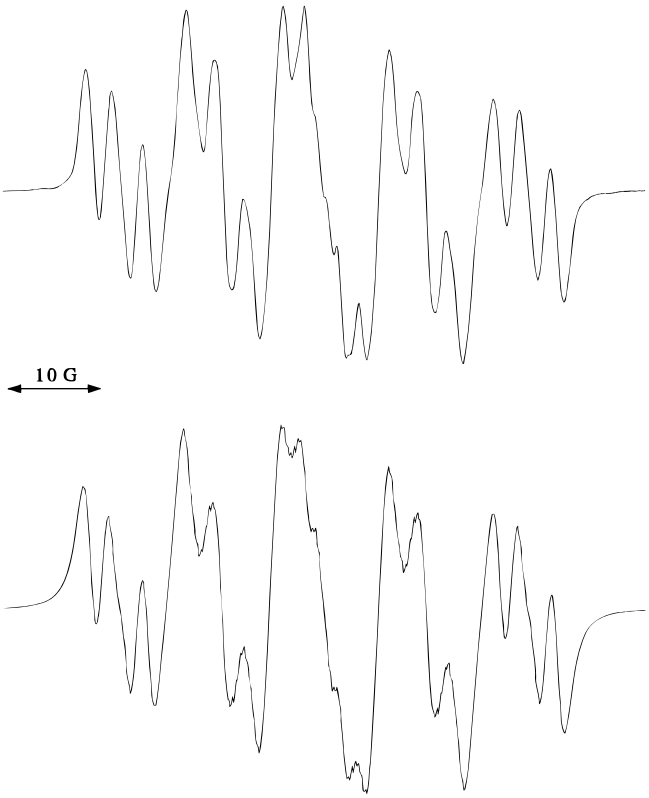

Figure 2. Comparison of the ESR spectrum of **aB6**σ^0 (top) with that of a simulation using the parameters listed in the text.

(5) Hush, N. S. *Coord. Chem. Rev.* **1985**, *64*, 135.

Table 3. CT Band Optical Data and Hush Analysis for Bis-diazenium Radical Cations

Four σ-Linked Compound[a]

	sBT$^+$		**aBT**$^+$	**aBH**$^+$	
solvent[b]	AN	MC[c]	AN	AN	DMF
λ_{max} (nm)	106_2	105_6	108_1	119_9	112_6
E_{op} (10^3cm^{-1})	9.42	9.47	9.25	8.34	8.88
E_{op} (kcal/mol)	26.9	27.1	26.4	23.8	25.4
ϵ (M^{-1} cm^{-1})	1450	1200	930[d]	1350	1225
$\Delta\nu_{1/2}$ (10^3cm^{-1})	6.50		7.03	6.80	7.31
Hush V_H (kcal/mol)	3.7		3.1[d]		3.4

Six σ-Linked Compound[e]

	sB6σ^+			**aB6**σ^+		
solvent[b]	AN	DMF	MC	AN	DMF	MC
λ_{max} (nm)	754(0)	746(0)	855(3)	761(3)	747(0)	871(3)
E_{op} (10^3cm^{-1})	13.26(0)	13.40(1)	11.70(4)	13.15(4)	13.39(0)	11.48(4)
E_{op} (kcal/mol)	37.92(0)	38.34(2)	33.47(12)	37.61(12)	38.30(0)	32.84(12)
ϵ (M^{-1} cm^{-1})	191(15)	177(4)	170(7)	198(11)	185(8)	171(14)
$\Delta\nu_{1/2}$ (10^3cm^{-1})	8.17(12)	7.85(11)	7.99(13)	7.87(20)	7.85(35)	7.14(18)
Hush V_H (kcal/mol)	1.18(4)	1.11(1)	1.03(3)	1.17(2)	1.14(2)	0.98(6)

[a] From ref 1a, but with V_H recalculated using the X-ray *d* of 4.733 Å for **BT**$^+$ (from **aBT**$^{2+}$, ref 1b) and 4.864 Å for **aBH**$^+$ (from **aBH**$^{2+}$, ref 1b). [b] AN = CH_3CN, DMF = *N*,*N*-dimethylformamide, MC = methylene chloride. [c] Methylene chloride showed an especially large high-frequency end second CT band, and we were unable to establish a reliable band width. Overlap of the two bands puts λ_{max} also in question. [d] V_H is low because of an anomalously small ϵ. If ϵ were 1400, V_H would be calculated at 3.8 kcal/mol. In retrospect, we do not doubt that ϵ was determined to be too small and that **s-** and **aBH**$^+$ have the same V_H, of about 3.7 kcal/mol. [e] Each entry shows the average of two separate samples, with the difference between the average and each determination in the last decimal place given in parentheses.

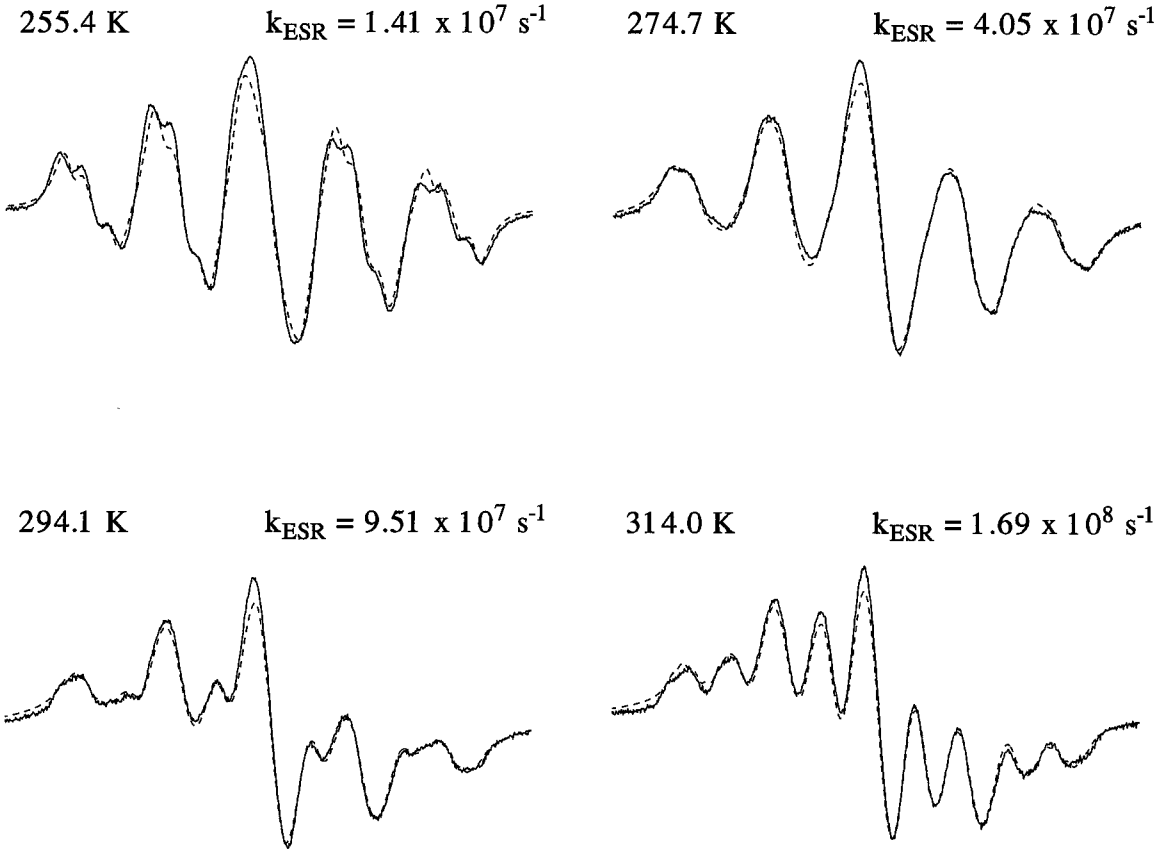

Figure 3. Comparison of experimental spectra for **aB6**σ^+ in acetonitrile (solid lines) at four temperatures with calculations using the simulation parameters shown in Table 7.

exchange rate for best fit to each spectrum. A sample of the fits obtained is shown in Figure 3. The dynamic ESR fits are certainly not perfect. At the lower temperatures required for the MC data to observe the localized, *a*(2N) spectrum, more broadening occurs in the $M_n \pm 2$ lines than fits the lines with smaller $|M_n|$ values, which is expected because of nonuniform line width effects for these bonded $I = 1$ nucleus spectra.[7] At the higher temperatures, where ET is fast enough that *a*(4N) spectra are observed, extra splitting is observed in the $M_n = \pm 4$ and ± 3 lines which is not simulated by the splitting constants

(6) Dovlaitzky, M.; Chiarelli, R.; Rassat, R. *Angew. Chem. Int. Ed. Engl.* **1992**, *31*, 180. They quote Hirota (Hirota, N., Weissman, S. I. *J. Am. Chem. Soc.* **1964**, *86*, 1538) as the source of the formula, although what is given there is the Hamiltonian used to derive it.

(7) Nelsen, S. F.; Echegoyen, L. *J. Am. Chem. Soc.* **1975**, *97*, 4930.

Table 4. k_{et} values From Dynamic ESR

solvent	*T* range (K)	$k_{ESR}(298)$ (10^7 s^{-1})[a]	$\Delta H^{\ddagger}$ (kcal/mol)[b]	$\Delta H^{\ddagger}$ (kcal/mol)[b]	k_{350}/k_{250} (ESR)	k_{ESR}/k_{cal} (298 K)[c]
			sB6σ^+			
AN	273−323(50)	11.5(7)	4.5(6)	−6.5(20)	19	5.8−7.3
DMF	293−333(50)	7.7(5)	4.8(6)	−6.5(20)	21	3.9−5.7
MC	214−293(79)	27(+13,−10)	4.0(11)	−10.5(34)	14	1.3−3.8
			aB6σ^+			
AN	236−254(118)	9.0(9)	5.2(4)	−4.9(14)	27	3.2−4.5
DMF	283−343(60)	7.9(4)	4.6(4)	−7.1(12)	19	4.5−5.1
MC[d]	214−293(79)	22(+11,−8)	3.6(10)	−8.4(42)	11	2.0−6.7
MC[d]	222−303(81)	23(+8,−6)	3.6(9)	−8.3(33)	11	2.5−6.3

[a] Ranges quoted are statistical error only (95% confidence) using the range in $\Delta G^{\ddagger}$ determined from the Eyring plot. [b] Numbers in parentheses are statistical error in the last place quoted (95% confidence, derived from the Eyring plot). [c] k_{cal} values taken from Table 5. The range quoted includes the extremes quoted for both k_{cal} and k_{ESR}. [d] Results of two separate runs, analyzed independently.

employed (most pronounced for the MC data). A summary of the rate constants obtained, including statistical error from an Eyring analysis, appears in Table 4, and the simulation parameters and rate constants appear in Table 7 (Experimental Section).

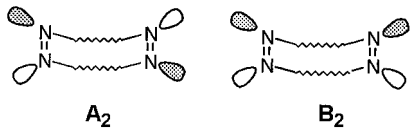

Discussion: *V* Values from PE Spectroscopy

Paddon-Row and co-workers pointed out that the antisymmetric π orbital combination ($\pi-\pi$) of **10(4**σ) has a 0.87 eV smaller vertical ionization potential (vIP) than that of the ($\pi+\pi$) symmetric combination because of the symmetry properties of the σ combination orbitals.[4] The ($\pi-\pi$) orbital exhibits much larger σ,π interaction, and hence destabilization for the ($\pi-\pi$) − σ_A combination orbital, than does the ($\pi+\pi$) − σ_S combination orbital. This occurs both because σ_A is the HOMO, so the energy gap is smaller, and because the principal interaction is between each π orbital and the allylic σ_{CC} hybrid orbital, and the orbital coefficients at the allylic carbons are much lower in the symmetric σ_S (HOMO-1), which can interact with ($\pi+\pi$), than they are in the σ_A HOMO, which interacts with ($\pi-\pi$). Hush equated this π combination orbital splitting with the twice the electron coupling (transfer) integral, *V*, employed in ET theory.[5] Thus, the gas phase V_{PE} value is given by eq 1 for these systems. The decrease in V_{PE} observed for

$$V_{PE} = (\mathrm{vIP}_2 - \mathrm{vIP}_1)/2 \qquad (1)$$

10(6σ) compared to that for **10(4**σ) is consistent with that seen for similar structural changes estimated by other methods.[5] Using a common formulation in which *n* is the number of σ bonds in a linking group, the decrease is expected to be exponential with *n*, according to eq 2.[5] For $\mathbf{10}^+$, $\beta(4 \rightarrow 6) = 0.50$ from Paddon-Row's data quoted in Table 1.

$$V = \mathrm{A}\exp^{-\beta n} \qquad (2)$$

The π_{NN} ionizations for the bis-azo compounds are buried in the σ ionization envelope, but the antisymmetric lone pair combination orbitals for each azo unit couple through the σ bond links, producing a lowest ionization band corresponding to formation of the cation having an A_2 symmetry SOMO, and a slightly higher vIP band corresponding to formation of its B_2 first excited state, as pictorially indicated below (using C_{2v} symmetry labels).[8] These bands contain unresolved vibrational splittings, but their maxima give the vIP values quoted in Table 1. It will be noted that the V_{PE} for $\mathbf{H}^+$ is only 73% as large as that for $\mathbf{T}^+$. The extra, longer σ-coupling pathways provided by the extra four- and five-membered rings present in **H** significantly lower *V* instead of raising it. Similar "interference" between multiple-coupling pathways has been observed in computations previously,[9] including between the cross-links in double linkers like Paddon-Row and we are using. The lower V_{PE} for $\mathbf{H}^+$ than for $\mathbf{T}^+$ is also predicted by the most simple analysis of semiempirical calculations,[10] as is V_{PE} for **10(4**σ)$^+$ lying between those for $\mathbf{H}^+$ and $\mathbf{T}^+$ (last column of Table 1). Despite the quite different geometry of the spin-bearing orbitals for the azo compounds (orbitals s-rich and in plane with the N−C bonds) and the olefins (orbitals nearly pure p and perpendicular to the C(sp^2)−C(sp^3) bonds), the observed V_{PE} values are only slightly larger for $\mathbf{T}^+$ than for **10(4**σ)$^+$ (11%) and for **6**σ^+ than **10(6**σ)$^+$ (5%). We note that $\beta(4\sigma \rightarrow 6\sigma)$ is the same within experimental error for bis-azo compounds $\mathbf{T}^+$ and **6**σ^+ (at 0.52), as that for **10(4**σ) → **10(6**σ).[10b]

V_{PE} values we have seen are substantially higher than any *V* values estimated from solution measurements. As pointed out to us by a referee, the wave functions representing two localized electronic states in a solvent are actually wave functions of the solute and the solvent. Matrix elements such as *V* can be less than those between the corresponding wave functions of the solute alone, because the solvent contributes an "electronic Franck-Condon factor".[11]

Discussion: CT Absorption Bands for Four- and Six-σ-Bond-Linked Bis-diazenium Cations

In our previous work on the $\mathbf{BT}^+$ diastereomers and $\mathbf{aBH}^+$, we observed an unexpected band overlapping with the low-energy side of the CT band. This band shifted with solvent (like) the main CT band and grew in intensity relative to the

(8) The *x,y* plane bisects the N=N bonds, the *y* direction is parallel to the longer axis, and the *z* direction is parallel to the N=N bonds.

(9) (a) Shepard, M. J.; Paddon-Row, M. N.; Jordan, K. D. *J. Am. Chem. Soc.* **1994**, *116*, 5328. (b) Jordan, K. D.; Paddon-Row, M. N. *Chem. Rev.* **1992**, *92*, 395.

(10) (a) Calculated V_{PE} values are quite sensitive to exactly what quantity is calculated. The $|E(\mathrm{HOMO}) - E(\mathrm{HOMO\text{-}1})|/2$ values, where *E* is the eigenvalue, tabulated in Table 1 represent the most naive assumption for calculating V_{PE}, which Koopmanns' theorem applies. More complex attempts, subtracting the enthalpy of neutral compound from enthalpies of the ground and first excited state radical cations with or without UHF treatment of the cations, and with or without their geometry optimization, agree no better with experiment, and some get the order wrong. They are more difficult to implement, especially because AM1 gets the state ordering wrong for $\mathbf{H}^+$. They also underestimate V_{PE}. (b) The V_{PE} calculated as in a above (last column of Table 1) obtain β for **10(4**σ)$^+$ → **10(6**σ)$^+$ significantly too large at 0.63 kcal/mol (AM1) and 0.68 kcal/mol (PM3).

(11) Young, R. H. *J. Chem. Phys.* **1992**, *97*, 8261.

Table 5. Vibronic coupling CT band analysis for *syn*- and *anti*-**B6**σ^{+a}

	sB6σ^+			**aB6**σ^+		
solvent[b]	AN	DMF	MC	AN	DMF	MC
λ (kcal/mol)	41.22(11)	41.57(6)	37.40(25)	40.80(15)	41.53(10)	36.18(11)
V_J (kcal/mol)	1.00(4)	0.95(1)	0.87(2)	1.01(2)	0.97(2)	0.82(4)
λ_s (kcal/mol)[c]	20.7(3)	19.9(10)	13.6(2)	19.9(9)	20.2(5)	[19.7(7)][d]
λ_v (kcal/mol)	20.5(4)	21.7(11)	23.8(4)	20.9(11)	21.3(6)	[16.4(8)][d]
$k_{cal}(298)$ ($10^7 s^{-1}$)	1.76(9)	1.65(21)	11.9(1.4)	2.34(14)	1.64(4)	[5.9(10)]
calcd k_{350}/k_{250}	31	29	12	28	30	[24]

[a] Each entry shows the average of two separate samples, with the difference between the average and each determination in the last decimal place given in parentheses. [b] AN = CH_3CN, DMF = *N*,*N*-dimethylformamide, MC = methylene chloride. [c] Reported for $h\nu_v$ = 3.15 kcal/mol (1100 cm^{-1}). [d] The λ_s,λ_v separation here is clearly anomalous, so quantities derived from these parameters are probably not correct; see text.

main band in some solvents (see ref 2a, Figures 2 and 3).[12] Neither **B6**σ^+ diastereomer shows much evidence for a similar second band in the CT region, except in MC (see below). The presence of the second band in four σ-linked systems precludes a reasonably precise Jortner theory CT band analysis, and we shall compare the four- and six σ-bond-linked systems using the Hush analysis shown in Table 3. The transition energy at the CT band maximum, E_{op} is equal to λ in Marcus/Hush theory, but λ is larger than E_{op}, using a Jortner analysis. Because the difference between λ and E_{op} is reasonably constant for the **B6**σ^+ diastereomers (see below) and we discuss differences between different compounds here, we shall employ E_{op}, which is known for both types of compounds. E_{op} is 2.85(25) kcal/mol larger for the **BT**$^+$ diastereomers than it is for **aBH**$^+$, which we attributed to the larger twist present in the center of the **BT**$^+$ systems, because twisting more at the NN bond of the reduced dinitrogen unit would increase λ_v.[2a] The increase in distance for **aBH**$^+$ compared to the **BT**$^+$ diastereomers should increase the solvent portion of the vertical reorganization energy, λ_s, for **aBH**$^+$. Using the Marcus dielectric continuum formula shown in eq 3 with the X-ray dinitrogen unit distances of the neutral *tert*-butyl, isopropyl-substituted hydrazines[13] as *d* predicts a 1.2 kcal/mol larger λ_s for **aBH**$^+$ in AN, so the difference in λ_v indicated by these data is about 4 kcal/mol. Because **6**σ is

$$\lambda_s(\text{kcal/mol}) = 332.1(r^{-1} - d^{-1})[(n_D{}^2)^{-1} - \epsilon^{-1}] \quad (3)$$

untwisted at the central CC bond, we believe that **aBH**$^+$ should be a better model for λ_v of the **B6**σ^+ diastereomers than are the **BT**$^+$ diastereomers. Using the dication X-ray distances which are available, 7.101 Å (**sB6**σ^{2+}), 5.076 (**aBH**$^{2+}$), and 4.915 (**aBT**$^{2+}$) with eq 3, λ_s(AN) is predicted to be 9.9 kcal/mol larger for **aB6**σ^+ than for **aBH**$^+$ (observed ΔE_{op} = 13.8 kcal/mol, calculated value 28% smaller), and 11.0 kcal/mol larger for **aB6**σ^+ than for **aBT**$^+$ (observed ΔE_{op} = 11.2 kcal/mol, but λ_v is less likely to be the same for these two compounds).

V in Hush theory is obtained from eq 4, using the molar absorptivity, ϵ_{max}, the band width at half height, $\Delta\nu_{1/2}$, and E_{op}.

$$V_H\,(\text{cm}^{-1}) = (2.06 \times 10^{-2})\,(\epsilon_{max}\Delta\nu_{1/2}E_{op})^{1/2}/d \quad (4)$$

Increasing the double link from four to six σ bonds decreases V_H from 3.7 kcal/mol for **sBT**$^+$ (as noted in Table 2, footnote *c*, we believe *V* is probably the same for the *anti* diastereomer) and 3.4 kcal/mol for **aBH**$^+$ to 1.18(1) kcal/mol for the **B6**σ^+ diastereomers. A smaller *V* for **H**-linked than for **B**-linked hydrazine radical cations has also been in the gas phase, as noted above, and in solution for bis-hydrazine systems,[13] so we suggest that the best comparison to make is between **sBT**$^+$ and the **B6**σ^+ diastereomers, which have quite similar links which differ by two σ-bonds. Using eq 2, *n* is 0.57 from Hush analysis of the optical spectra of these compounds. As might be expected from the similarity in linking structure, this is consistent with the β = 0.60 obtained from fluorescence lifetime measurements on photoexcited **12(6**σ**)** and **12(4**σ**)**.[14] It is larger than the 0.50

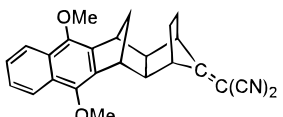

12(4σ)

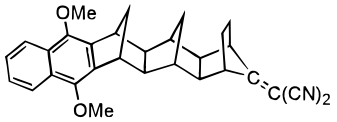

12(6σ)

from V_{PE} of **10(6**σ**)** and **10(4**σ**)**.[5] Our V_H(**B6**σ^+) = 1.2 kcal/mol is significantly larger than that obtained from fluorescence quenching rate constants for **12(6**σ**)**, *V* = 0.32 kcal/mol.[14] It has subsequently been pointed out that most of the CT fluorescene band intensity for **12(n**σ**)** and related compounds arises from mixing of the CT state with the locally excited one, making the observed "*V**" much larger than the true *V*,[15] which presumably makes agreement even poorer.

Discussion: Jortner Theory ET Parameters for B6σ^+

Because the **B6**σ^+ bis-diazenium cations have a single CT band, we could also analyze them by simulation, using Jortner vibronic coupling theory.[16] We used a single coupling frequency energy ($h\nu_v$) form, employing the Kodak group's equations,[17] as discussed in detail for similar analysis of bis-hydrazine radical cations **13**$^+$ and both diastereomers of **14**$^+$ in the accompanying paper.[13] The results are shown in Table 5.

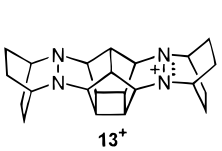

13$^+$

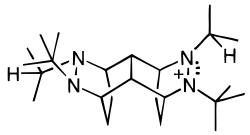

s14$^+$

(12) (a) We have attributed[12b] this second band to a minor conformation present at the reduced (diazenyl oxidation level) dinitrogen unit on the basis of AM1 calculations which predict a very small energy difference betwen the two nitrogen inversion forms but nevertheless a significant effect upon the vertical vibrational reorganization energy (λ_v), because pyramidality at the nitrogens in the two inversion forms is slightly different, and λ_v is predicted to be exceptionally sensitive to this difference. (b) Nelsen, S. F. *J. Am. Chem. Soc.* **1996**, *118*, 2047.

(13) (a) Nelsen, S. F.; Ramm, M. T.; Wolff, J. J.; Powell, D. R. *J. Am. Chem. Soc.* **1997**, *119*, xxxx. (b) See ref 13a, footnote 14. (c) DMF also leads to higher λ than AN for the four σ-bond-bridged **BH**$^+$ (see Table 3) and for both diastereomers of hydrazines **14**$^+$. For **14**$^+$, where $\Delta E°$ is large enough to determine more accurately than it is for the six σ-bond-linked bis-diazeniums, the electrochemistry indicated that DMF specifically stabilizes oxidized hydrazine units relative to AN more than expected from eq 3.[13a]

(14) Oevering, H.; Paddon-Row, M. N.; Heppener, M.; Oliver, A. M.; Cotsaris, E.; Verhoeven, J. W.; Hush, N. S. *J. Am. Chem. Soc.* **1987**, *109*, 3285.

(15) Bixon, M.; Jortner, J.; Verhoeven, J. W. *J. Am. Chem. Soc.* **1994**, *116*, 7349.

(16) Ulstrup, J.; Jortner, J. *J. Chem. Phys.* **1975**, *63*, 4358.

(17) Gould, I. R.; Noukakis, D.; Gomez-Jahn, L.; Young, R. H.; Goodman, J. L.; Farid, S. *Chem. Phys.* **1993**, *176*, 439.

Table 6. Comparison of ESR-Derived Intermolecular ET Rate Constants with Theory for Bis-diazenium and Bis-hydrazine Radical Cations

cmpd	charge-bearing unit	solvent	k_{ESR}/k_{cal} (298 K)	ESR (k_{350}/k_{250})	calcd (k_{350}/k_{250})	$S = \lambda_v/h\nu_v$
13^{+} [a]	*cis* hydrazine$^{\bullet+}$	CH_3CN	20	2.1	53	17.5
14^{+} [b,c]	*trans* hydrazine$^{\bullet+}$	CH_2Cl_2	23, 26	9.6, 9.1	71, 76	14.1, 13.5
B6σ^{+} [c]	diazenium^{+}	CH_3CN	5.8, 5.3	19, 27	31, 28	6.5, 6.6
		DMF	4.7, 4.8	21, 19	29, 30	6.9, 6.8
		CH_2Cl_2	2.5, d	14, 11	12, *d*	7.6 *d*

[a] Data from ref 7, Tables 4 and 6. [b] Data from ref 7, Tables 2 and 3. [c] Data listed for *syn*, followed by *anti* diastereomer. [d] Entry lacking because of problems with the λ_s,λ_v separation.

In this analysis, λ is determined by the band shape and the electronic coupling, V_J, is systematically smaller than V_H (as it is typically employed)[13b] but close to $V_H = n_D^{1/2}V_J$ (where n_D is the refractive index of the solvent; compare the entries in Tables 3 and 5). Comfortingly, the V_J values are nearly the same for the two diastereomers in each solvent, the maximum difference being in MC, where the *syn* diastereomer gave λ 1.2 kcal/mol larger and V_J <0.1 kcal/mol larger than the *anti* one. It may be noted from Figure 1 that there is a slight bulge on the low-energy side of the observed CT band compared to the calculated one in MC; this might be related to the second band observed for the four σ-bond-bridged systems which was mentioned above. We have attempted to ignore the bulges, which are only distinctly seen in MC. The λ_s,λ_v separation using vibronic coupling theory is strongly dependent upon the hν_v value which is employed, and use of larger $h\nu_v$ values increases the λ_s value required for fit. The bis-hydrazine radical cations[13] should have significantly smaller $h\nu_v$ values than the bis-diazenium radical cations studied here: the former includes R_2-NNR_2^0 (single bond) and $R_2NNR_2^+$ (3e π-bond) stretches and the latter R_2NNR^0 (3e π-bond) and R_2NNR^+ (double bond) stretches, and their values are significantly different.[10] Somewhat more quantitatively, dynamic reaction coordinate (DRC) semiempirical calculations using AM1-UHF[10] predicted averaged $h\nu_v$ of 2.36 kcal/mol (827 cm^{-1}) for **13**$^{+}$, and a value even somewhat lower than this was most consistent with the λ_s,λ_v separation obtained from Jortner analysis of its CT band if λ_s is considered to be reasonably estimated using dielectric continuum theory.[13] These calculations predict $h\nu_v$ of about 4.00 kcal/mol (1400 cm^{-1}) for **sBT**$^{+}$ and about 3.72 kcal/mol (1300 cm^{-1}) for **aBT**$^{+}$, both a surprisingly large difference, and probably too high; the AM1 frequencies are not very good.[10] Unpublished resonance Raman experiments by Hupp and Williams[18] give relative contributions and frequencies active for ET which gave weighted average $h\nu_v$ values of ca. 3.29 and 3.20 kcal/mol (1150 and 1120 cm^{-1}), respectively, and we have analyzed the CT band absorption spectra data in Table 5 using $h\nu_v = 3.15$ kcal/mol (1100 cm^{-1}) for this reason. The best fits to the CT band absorption curves occur for λ_v which averages to 21.7 (range +2.5, −1.0) kcal/mol for five of the six spectra examined. Something appears to be wrong with our **aB6**σ^{+} in MC analysis, which gives an anomalous λ_s,λ_v partitioning. The partitioning obtained is sensitive to small changes in the wings of the spectrum, as discussed in more detail for the bis-hydrazine data set,[13] where similar problems also occur. As pointed out above, E_{op}(AN) for these six σ-bond-linked bis-diazenium radical cations is about 13.8 kcal/mol higher than their four σ-bond-linked **BT**$^{+}$ analogues, compared to the dielectric continuum approximation (eq 3) prediction of an increase of λ_s(AN) of 11.6 kcal/mol. Increasing the $h\nu_v$ used for analysis raises λ_s and lowers λ_v. For example, if $h\nu_v = 3.30$ kcal/mol (1155 cm^{-1}) is used for analysis of the **s6B**σ^{+} band in AN, λ_s is increased by 1.35 kcal/mol and λ_v is lowered by 1.32 kcal/mol. We suspect that there is at least a 2 kcal/mol uncertainty in the partitioning of λ into λ_s and λ_v using CT band simulation under the best of circumstances for our compounds, but suggest that using $h\nu_v$ of 3.15 kcal/mol (or a little larger) leads to reasonable values for λ_s(AN) and λ_v values for these compounds. Expecting to quantitatively separate λ_s from λ_v using λ vs γ plots and eq 3 is unreasonable, because as it is for the related bis-hydrazines,[13] λ is higher in DMF than in AN for these bis-diazenes. The rate constants expected from Jortner theory for the **B6**σ^{+} diasteromers using the parameters obtained from the CT bands are also shown in Table 5; for the equations used and more discussion, see the accompanying paper.[13]

Discussion: Comparison of Calculated and Observed Rate Constants

Comparison of the calculated rate constants at 298 K with those observed by dynamic ESR (interpolated to 298 K) is made Table 4.[19] All of the observed rate constants are higher than the calculated ones, but agreement is rather good, with the average ratio being under 7 for data in all three solvents, for both diastereomers. An important test of the agreement of theory with experiment involves the temperature sensitivity of k_{et}. The activation parameters from the ESR experiments give ESR k_{350}/k_{250} ratios of 19−27 in AN and DMF and somewhat smaller ratios of 11−14 in MC (see Table 4). Jortner theory using the ET parameters derived as described from the CT bands give ratios of 28−31 for AN and DMF and 12 for **sB6**σ^{+} MC (as pointed out above, for **aB6**σ^{+}, the MC ET parameters obtained from the CT band are anomalous). Agreement of the predicted temperature sensitivity with experiment is also rather good.

Conclusions

There is greater difficulty in measuring dynamic ESR rate constants for bis-diazenium than for bis-hydrazine radical cations because bis-diazeniums are less close to being symmetrical within one spin-bearing dinitrogen unit, so their ESR spectra are more complex. Nevertheless, the k_{ESR} values obtained for the **B6**σ^{+} diasteromers studied here unquestionably fit Jortner theory predictions better than those for the bis-hydrazine radical cations, for which the best data are for the *cis* hydrazine unit perbicyclic compound **13**$^{+}$ in AN and the *trans* hydrazine unit *syn*- and *anti*-*t*-Bu,*i*-Pr compounds **14**$^{+}$ in MC,[13] as summarized in Table 6.[20] The entries for **14**$^{+}$ and **B6**σ^{+} include both *syn*

(18) R. Williams, J. T. Hupp, M. T. Ramm, and S. F. Nelsen, unpublished results.

(19) For completeness, we estimate k_{cal} using the Hush-theory-derived ET parameters for **sB6**σ^{+} in AN (Table 3). Using the observed $\Delta\nu_{1/2}$ with eq 28,[5] the Hush $h\nu_v$ is only 2.52 kcal/mol (880 cm^{-1}; anomalously small). We employed $\lambda_s = 50.2\%$ of E_{op} (the ratio arrived at in the Jortner analysis) (i.e., 19.04 kcal/mol). Using eqs 7−9 of ref 13, $k_{ad} = 2.2 \times 10^8$ s^{-1}, but using eq 69 of Sutin (Sutin, N. *Prog. Inorg. Chem.* **1983**, *30*, 441), the electronic transmission coefficient, $\kappa_{el} = 0.65$, leading to k_{cal}(Hush theory) $= 1.5 \times 10^8$ s^{-1}, which is close to the observed k_{ESR} of 1.15(7) $\times 10^8$ (Table 4). Thus, as for the bis-hydrazines,[13] using Hush theory parameters and adiabatic rate equations leads to slightly higher k_{cal} than the observed k_{ESR} values.

(20) As in previous work, we do not try to include temperature variation of the ET parameters, because we do not even know what direction to try to vary them and dielectric continuum theory is clearly inadequate to rationalize λ_s.

and *anti* diastereomers, because we believe that the differences are likely to reflect experimental error in determining the rate constants and ET parameters used in estimating the calculated rate constants more than real differences between the diastereomers, although the possibility that the diastereomers really do have slightly different values cannot be excluded. A possible conformational reason for the *cis* hydrazine unit compound $\mathbf{13}^+$ having so much smaller an ESR k_{350}/k_{250} ratio than the *trans* hydrazines $\mathbf{14}^+$ will not be repeated here.[13] The better fit to theory for $\mathbf{B6}\sigma^+$ than $\mathbf{14}^+$ may well be related to the size of the vibronic coupling constant $S = \lambda_v/h\nu_v$. As discussed in the accompanying paper,[13] the CT band analysis involves the $0 \rightarrow (w \text{ near } S)$ transitions, while the thermal barrier is only affected by transitions between $v,w \leq 4$, with $v,w = 0-2$ greatly predominating. Because S is about twice as large for the hydrazines as for the diazeniums, it seem reasonable that any anharmonicity present would affect the hydrazine data considerably more. We hope to probe this in the future experimentally, by making systems with other S values and by carrying out variable temperature studies of the CT bands to determine whether or not the constant ET parameters we used here in comparing the temperature effects are a reasonably good assumption.

Experimental Section

Instrumentation. NMR spectra were recorded on a Bruker AM-300 spectrometer. ESR spectra were taken on a Bruker ESP 300E spectrometer. All NMR spectra were taken in CD_3Cl_3 except where noted. UV−vis spectra were taken on a Hewlett-Packard 8452A diode array spectrophotometer using matched 1 cm quartz cells. Near IR spectra were recorded on a Nicolet 740 spectrophotometer using Pb/Se and red-filtered Si detectors with matched 1 cm quartz cells. Photoelectron spectra were acquired using a Varian IEE-15 instrument. Electrochemistry was carried out using an EG&G PAR Model 273 interfaced to a Dell 386, using M270 software.

1,5,6,7,8,12,13,14-Octachloro-15,15,17,17-tetramethoxyhexacyclo[10.2.1.1^{3,10}.1^{5,8}.0^{2,11}.0^{4,9}]heptadeca-6,13-diene (3). A solution of 5,5-dimethyoxytetrachlorocyclopentadiene (50.00 g, 189 mmol), norbornadiene (10.2 mL, 94.7 mmol), and chlorobenzene (70 mL) was refluxed for 23 h, and the solution filtered after cooling to 0 °C, resulting in **3** as white needles (34.47 g) after washing with hexanes and drying at 0.1 mm Hg; mp 288−290 °C (lit.[21] mp 287 °C). A second crop of crystals (2.86 g) with the same melting point was obtained by dilution of the mother liquors with hexanes: combined yield 40.33 g (69%); ^{1}H NMR δ 1.11 (brs, 2H), 2.43 (brs, 4H), 2.52 (brt, J = 1.6 Hz, 2H), 3.50 (s, 6H), 3.60 (s, 6H).

15,15,17,17-Tetramethoxyhexacyclo[10.2.1.1^{3,10}.1^{5,8}.0^{2,11}.0^{4,9}]-heptadeca-6,13-diene (4). *tert*-Butyl alcohol (120 mL) was added to **3** (20.00 g, 32.26 mmol) in THF (250 mL), resulting in some precipitation. While the solution was stirring, finely cut sodium (40.0 g, 1.74 mol) was added, and the mixture was slowly heated to reflux under N_2 and refluxed for 48 h. During the first hour, the solution turned purple. After the solution had cooled to room temperature, methanol (30 mL) was added, and the solution was stirred for 30 min under N_2. The large pieces of sodium were removed and destroyed separately with methanol. The methanol solution and the remaining purple solution were combined and carefully poured into 600 mL of water, resulting in discharge of the purple color. The aqueous solution was diluted to 1.2 L with water and extracted with methylene chloride (4 × 120 mL). The combined organic phases were washed with water (3 × 200 mL) and saturated aqueous NaCl (100 mL) and dried with $MgSO_4$. After the solvent was evaporated and the residue dried at 0.1 mm Hg, a white solid (10.95 g) was left. Recrystallization from isooctane gave **4** as colorless prisms (6.67 g, 60.0%): ^{1}H NMR δ 1.71 (br pentet, J = 1.5 Hz, 2H), 2.01 (m, 6H), 2.85 (pseudopentet, J = 2.1 Hz, 4H), 3.04 (s, 6H), 3.18 (s, 6H), 5.91 (t, J = 2.4 Hz, 4H); ^{13}C NMR δ 32.78, 39.67, 48.21, 48.51, 49.54, 51.97, 121.70, 132.51; HR-MS ($C_{21}H_{28}O_4$) calcd 344.1987, found 344.1985 (M^+, 30%).

Hexacyclo[10.2.1.1^{3,10}.1^{5,8}.0^{2,11}.0^{4,9}]heptadeca-6,13-diene-15,17-dione (5). A solution of **4** (4.34 g, 12.6 mmol), 70% $HClO_4$ (10.5 mL), water (21 mL), and THF (120 mL) was stirred at room temperature under N_2 for 14 h, the mixture was poured into water (500 mL), and the resulting precipitate was collected by filtration. The solid was dissolved in CH_2Cl_2 (50 mL), the resulting solution was washed with saturated aqueous $NaHCO_3$, and the organic phase was dried over $MgSO_4$. Rotary evaporation of the solvent at room temperature gave **5** as a white solid (2.89 g, 90.3%); mp (dec.) 118 °C. This material was pure by ^{1}H NMR. For **5**: ^{1}H NMR δ 1.63 (brt, J = 1.5 Hz, 4H), 2.13 (pseudotriplet, J = 2.2 Hz, 4H), 2.53 (brt, J = 1.4 Hz, 2H), 3.08 (pentet, J = 2.3 Hz, 4H), 6.31 (pseudotriplet, J = 2.5 Hz, 4H); ^{13}C NMR δ 33.90, 44.07, 44.70, 51.34, 130.54, 198.58.

Tetracyclo[6.6.1.0^{2,7}.0^{9,14}]pentadeca-3,5,10,12-tetraene (6). A clear colorless solution of **5** (2.89 g, 11.45 mmol) in THF (50 mL) was refluxed under N_2 for 14 h, and the solvent was removed by rotary evaporator to give an off-white solid (2.35 g) which was recrystallized from hot isooctane. Four crops of colorless leaflets (1.90 g total, 76.9%) with identical melting points (mp = 127−129 °C were collected. For elemental analysis, a small portion was recrystallized to give leaflets with an mp of 129−130.5 °C. For **6**: ^{1}H NMR δ 1.85 (m, 2H), 1.90 (m 2H), 2.71 (m, 4H); 5.32−5.40 (m, 4H), 5.52−5.61 (m, 4H); ^{13}C NMR δ 31.44, 44.26, 55.49, 121.74, 128.05; HR-MS ($C_{15}H_{16}$) calcd 196.1252, found 196.1256 (M^+, 36%). Anal. Calcd for $C_{15}H_{16}$: C, 91.78; H, 8.22. Found C, 91.53; H, 8.15.

Bis(*N*-methyltriazolinedione) adduct of 6 (8). A solution of *N*-methyltriazolinedione (2.19 g, 19.4 mmol) in CH_2Cl_2 (40 mL) was added via cannula to a stirred, 0 °C solution of **6** (1.90 g, 9.68 mmol) in CH_2Cl_2 (30 mL). The solution was stirred for 1 h at 0 °C, the solvent was evaporated, and the residue was carefully washed with acetone (3×) and isooctane, giving **8** (3.50 g, 85.6%) as a single symmetrical stereoisomer with mp > 300 °C (dec., darkens from 200 °C onward). For **8**: ^{1}H NMR δ 1.62 (brs, 2H), 2.14 (brs, 2H), 2.23 (m, 4H), 2.92 (s, 6H), 4.85 (m, 4H), 6.20 (dd, J = 3.2, 4.2 Hz, 4H); ^{13}C NMR δ 25.31, 28.65, 40.25, 45.55, 53.06, 129.97, 158.00; HR-MS ($C_{21}H_{22}N_6O_4$) calcd 422.1702, found 422.1722 (M^+, 4%).

Hydrogenation of 8. A stirring suspension of **8** (0.94 g, 2.2 mmol) and 5% Pd/C (0.25 g) in acetic acid (100 mL) was hydrogenated at room temperature and atmospheric pressure for 18 h. The suspension was filtered through Celite, and the catalyst was carefully washed with CH_2Cl_2. Recrystallization of the residue from CH_2Cl_2/hexane afforded **9** as a white solid (0.94 g, 98.9%): mp > 300 °C; ^{1}H NMR δ 1.78−1.99 (m, 14H), 2.24 (brs, 2H), 3.05 (s, 6H), 4.27 (brs, 4H); HR-MS ($C_{21}H_{26}N_6O_4$) calcd 426.2015, found 426.2021 (M^+, 100%).

4,5,11,12-Tetraazatetracyclo[6.6.1.0^{2,7}.0^{9,14}]pentadeca-3,5,-10,12-tetraene (6σ). A suspension of **9** (0.94 g, 2.2 mmol), KOH (2.7 g, 48 mmol), *i*-PrOH (40 mL), and water (10 mL) was refluxed under N_2 with vigorous stirring for 33 h. The solution was cooled in an ice bath, and the pH adjusted to 1 with concentrated HCl (CO_2 evolution). The solution was stirred at room temperature for 1 h, and a solution of $CuCl_2 \cdot 2H_2O$ (6.3 g) in water (20 mL) was added, resulting in formation

(21) MacKenzie, K. *J. Am. Chem. Soc.* **1960**, *82*, 473.

Table 7. Simulation Parameters and Rate Constants Used for Dynamic ESR Fits

cmpd	solvent	T (K)	a(N) G		a(H)		LW (G)	k_{ESR} ($10^7 s^{-1}$)	$\Delta G^{\ddagger}$ (kcal/mol)
sB6σ^+	CH_3CN	273	11.7	10.6	3.3	2.0	1.3	4.85	
		283	11.7	10.6	3.3	2.0	1.3	7.75	
		293	11.7	10.6	3.3	2.0	1.3	10.2	
		303	11.8	10.5	3.3	2.0	1.3	13.7	
		313	11.8	10.6	3.3	2.0	1.3	17.6	
		323	11.8	10.5	3.3	2.0	1.3	21.1	6.46(3)
	DMF	283	11.8	10.6	3.6	2.2	1.3	4.93	
		293	11.8	10.6	3.6	2.2	1.3	5.99	
		303	11.6	10.8	3.6	2.2	1.5	8.98	
		313	11.6	10.8	3.6	2.2	1.5	12.2	
		323	11.8	10.6	3.2	2.6	1.5	16.0	
		333	11.7	10.7	3.2	2.6	1.5	19.4	6.70(4)
	CH_2Cl_2	214	11.5	11.0	3.2	2.2	1.3	1.41	
		234	11.5	11.0	3.2	2.2	1.3	2.47	
		254	11.6	10.7	3.4	2.4	1.3	8.63	
		274	11.5	10.8	3.4	2.4	1.3	15.0	
		293	11.5	10.8	3.4	2.4	1.3	20.2	5.96(25)
aB6σ^+	CH_3CN	236	11.6	10.8	3.3	2.0	1.3	0.708	
		246	11.6	10.8	3.3	2.0	1.3	1.06	
		255	11.6	10.8	3.3	2.0	1.3	1.41	
		265	11.8	10.6	3.2	2.2	1.3	2.82	
		275	11.8	10.6	3.2	2.2	1.3	4.05	
		284	11.8	10.6	3.2	2.2	1.3	6.34	
		294	11.8	10.6	3.2	2.2	1.3	9.51	
		304	11.8	10.6	3.2	2.2	1.3	13.0	
		314	11.8	10.6	3.2	2.2	1.3	16.9	
		324	11.8	10.6	3.2	2.2	1.3	21.5	
		334	11.8	10.6	3.2	2.2	1.3	24.7	
		344	11.8	10.6	3.2	2.2	1.3	28.2	
		354	11.8	10.6	3.2	2.2	1.3	33.5	6.60(6)
	DMF	283	11.8	10.6	3.6	2.2	1.3	5.11	
		293	11.8	10.6	3.6	2.2	1.3	6.52	
		303	11.6	10.8	3.4	2.0	1.5	9.33	
		313	11.6	10.8	3.6	2.2	1.3	12.3	
		323	11.8	10.6	3.2	2.6	1.3	16.6	
		333	11.8	10.6	3.2	2.6	1.3	20.2	
		343	11.8	10.6	3.2	2.6	1.3	23.8	6.68(3)
	CH_2Cl_2	214	11.5	11.0	3.2	2.2	1.3	1.68	
		234	11.5	11.0	3.2	2.2	1.3	2.47	
		254	11.5	11.0	3.4	2.4	1.3	7.57	
		274	11.8	10.8	3.4	2.4	1.3	13.2	
		293	11.9	10.7	3.0	2.6	1.3	18.5	6.07(24)
	CH_2Cl_2	222	11.5	11.0	3.2	2.2	1.3	1.94	
		243	11.5	11.0	3.2	2.2	1.3	5.11	
		263	11.6	11.0	3.4	2.4	1.3	10.9	
		283	11.7	11.0	3.4	2.4	1.3	16.9	
		304	11.7	11.0	3.4	2.4	1.3	22.2	6.04(17)

of a brown precipitate. The mixture was stirred for 30 min and concentrated NH_4OH added, and the blue solution was extracted with CH_2Cl_2 (4 × 50 mL). The combined organic phases were washed with water (3 × 50 mL) and saturated aqueous NaCl and dried with $MgSO_4$. The residue, after solvent removal (0.58 g), was recrystallized from CH_2Cl_2/hexane. Three crops of a white powder (0.48 g total, 85%) were collected, which decomposed at 250 °C without melting. **For 6**σ: ^{1}H NMR δ 1.05−1.26 (m, 8H), 1.56−1.70 (m, 4H), 1.83 (brs, 2H), 2.04 (t, J = 1.4 Hz, 2H), 5.00 (brm, 4H); ^{13}C NMR δ 17.64, 30.09, 36.60, 41.90, 63.92.

4,11- and 4,12-Di-*tert*-butyl-4,5,11,12-tetraazatetracyclo-[6.6.1.0^{2,7}.0^{9,14}]pentadeca-3,5,10,12-tetraene Dication Bis(tetrafluoroborate) (s- and aB6σ^{2+}(BF$_4^-$)$_2$). A solution of **6**σ (1.00 g, 3.90 mmol), *t*-BuOH (150 mL), and HBF_4·OEt_2 (4.00 mL, 14.2 mmol) was refluxed under N_2 for 48 h. Filtration of the hot solution yielded a yellow-white solid (0.86 g) which ^{1}H NMR analysis showed contained **sB6**σ^{2+} with a small amount of **aB6**σ^{2+}. Recrystallization from CH_3CN/*i*-PrOH and solvent removal at 0.1 mm Hg gave **sB6**σ^{2+}(BF$_4^-$)$_2$ as a white powder, yield = 0.63 g (30%). The mother liquor was diluted with ether and filtered, giving 0.76 g of a white solid, which was recrystallized from CH_3CN/*i*-PrOH to give pure **a6**σ^{2+}(BF$_4^-$)$_2$, yield 0.56 g (26%). **sB6**σ^{2+}: mp (dec.) 245−246 °C; ^{1}H NMR (CD_3CN) δ 1.43−1.49 (m, 4H), 1.62 (s,2H), 1.65 (s, 18H), 1.90−1.95 (m, 5H), 2.14−2.21 (d, 4H), 2.60 (s, 2H), 5.73 (s, 2H), 5.90 (s, 2H); ^{13}C NMR (CD_3CN) δ 19.80, 22.62, 26.41, 30.84, 37.49, 38.21, 43.38, 45.81, 67.79, 72.03, 81.69. For **aB6**σ^{2+}: mp (dec) 244−246 °C; ^{1}H NMR (CD_3CN) δ 1.44−1.48 (d, 2H), 1.59 (m, 4H), 1.65 (s, 18H), 1.91−1.95 (m, 5H), 2.17−2.21 (d, 4H), 2.61 (s, 2H), 5.74 (s, 2H), 5.88 (s, 2H); ^{13}C NMR (CD_3CN) δ 19.90, 22.57, 26.45, 30.98, 37.96, 43.29, 46.14, 67.88, 72.10, 81.79.

Electrochemistry. The supporting electrolyte tetrabutylammonium perchlorate was recrystallized from hot ethanol/water and dried at 110 °C and 0.1 mm Hg. All solvents were distilled from an appropriate drying agent, stored over 3 Å sieves, and passed through dry, basic alumina prior to use. The cyclic voltammetry samples were 1 mM in analyte and 0.1 M in supporting electrolyte. Electrodes were polished immediately before use using 5 and 0.3 μm alumina. The reference electrode was a Corning ceramic junction SCE, the working electrode was a platinum disk electrode, and a silver wire was used as the counterelectrode. The coulometry cell consisted of a Pt

mesh electrode as the working electrode and silver wires as the reference and counterelectrodes. The counterelectrode was separated from the bulk of the solution by two glass frits that were separated by 1 cm from each other. Coulometric solutions consisted of 1−3 mM analyte and 0.1 M electrolyte. The electrolyte solution (no analyte) was degassed with Ar for 20 min and then electrolyzed while stirring by applying a constant potential of −1.0 V (vs Ag) until the current dropped to a minimum. The analyte was added, and the solutions were degassed with Argon for 20 min. The solutions were then electrolyzed by once again applying a constant potential of −1.0 V (vs Ag) while stirring. Electrolysis was stopped when the appropriate amount of charge had been passed.

X-ray Crystallographic Structure of 6σ. Crystals were grown by sublimation. The structure was determined at 113(2) K using a 0.4 × 0.4 × 0.2 mm crystal, on a Siemens P3f diffractometer using graphite-monochromated Cu Kα radiation (λ = 1.541 78 Å), Wyckoff scan type, θ range 2.00 to 57.00°. The solution of the structure with direct methods used program SHELXS-86 and the refinement used SHELXL-93, which refines on F^2 values.[22] **6**σ ($C_{15}H_{20}N_4$, fw256.35) crystals are monoclinic, space group C_2/m, with unit cell dimensions of a = 8.352(2), b = 10.2231(10), and c = 14.2308(10) Å, β = 97.974(8)°, V = 1203.3(3) Å^3, Z = 4, d_{calcd} = 1.415 mg/m^3, absorption coefficient = 0.683 mm^{-1}, and F(000) = 552. The number of reflections collected = 1844, independent reflections 865 [R(int) = 0.0438], data = 865, restraints = 0, parameters = 89, goodness-of-fit on F^2 = 1.098, final R indices R_1/wR2 = 0.0471/0.1182, R indices (all data) R_1/wR2 = 0.0534, 0.1210, extinction coefficient 0.0013(3), and largest difference peak/hole = 0.276/−0.290 eÅ^{-3}.[23]

X-ray Crystallographic Structure of sB6σ^{2+} (Ph_4B^-)$_2$ CH_3CN. Crystals were grown by vapor diffusion of ether into an AN solution. The structure was determined at 133(2) K using a 0.44 × 0.40 × 0.32 mm crystal, on a Siemens P4/CCD diffractometer using graphite-monochromated Mo Kα radiation (λ = 0.710 73 Å), using ϕ scan frame, θ range 1.73−28.23°. The solution of the structure with direct methods and the refinement used SHELXTL version 5, which refines on F^2 values.[22d] The crystals $((C_{23}H_{38}N_4)^{2+}2(C_{24}H_{20}B)^-(C_2H_3N)$, fw 1050.05) are triclinic, space group $P\bar{1}$, with unit cell dimensions of a = 11.2781(2), b = 12.2227(2), c = 22.9825(2) Å, α = 79.030(2), β = 76.686(2), γ = 76.421(2)°, V 2965.34(8) Å^3, Z = 2, d_{calcd} = 1.176 mg/m^3, absorption coefficient = 0.068 mm^{-1}, F(000) = 1128. Reflections collected = 29259, independent reflections 12717 [R(int) = 0.0370], data = 12717, restraints = 338(disorder), parameters = 994, goodness-of-fit on F^2 = 1.023, final R indices R_1/wR2 = 0.0490/0.0979, R indices (all data) R_1/wR2 = 0.0910, 0.1138, extinction coefficient 0.0035(4), and largest difference peak/hole = 0.271/−0.299 eÅ^{-3}.[23]

Dynamic ESR temperatures were determined using a Fluka Model 51 thermometer equipped with an 80PK-4A type K air probe. The sample and thermocouple were allowed to equilibrate in the ESR probe for 15 m before measurements were taken. Temperatures were within a few tenths of a degree of those registed by the spectrometer thermocouple. Spectral simulations employed program ESREXN by J. Heinzer, QCPE program 209, with modifications by Peter A. Petillo and Rustem F. Ismagilov to run on IBM-PC clones and a Unix computer (IBM RS-6000). Table 7 contains a list of the simulation parameters used and the exchange rate constants for each compound, solvent, and temperature studied in this work; the activation parameters derived from them appears in Table 4.

Calculations. AM1[24a] and PM3[24b] calculations were carried out using the VAMP programs.[25]

Acknowledgment. We thank the National Science Foundation for partial financial support of this research under Grant CHE 9417946 and the National Science Foundation, the National Institutes of Health, and the University of Wisconsin for funds used in purchasing the spectrometers and computers used in this work. We thank NATO for a travel grant which allowed the participation of J.J.W. in the synthetic work. We are especially indebted to Ralph Young (Kodak) for helpful discussions and to an exceptionally helpful referee.

JA9634177

(22) (a) Sheldrick, G. M. *Acta Crystallogr.* **1990**, *A46*, 467. (b) Sheldrick, G. M. Manuscript in preparation. (c) Neutral atom scattering factors were taken from *International Tables for Crystallography*; Kluwer:Boston, 1992; Vol. C, Tables 6.1.1.4, 4.2.6.8, 4.2.4.2. (d) SHELXTL version 5 Reference Manual, Siemens Analytical X-ray Instruments, 6300 Enterprise Dr., Madison, WI 53719-1173.

(23) The authors have deposited atomic coordinates for this structure with the Cambridge Crystallographic Data Centre. The coordinates can be obtained, on request, from the Director, Cambridge Crystallographic Data Centre, 12 Union Road, Cambridge, CB2 1EZ, U.K.

(24) (a) For AM1, see: Dewar, M. J. S.; Zoebisch, E. G.; Healey, E. F.; Stewart, J. J. P. *J. Am. Chem. Soc.* **1985**, *107*, 3902. (b) For MNDO-PM3, see: Stewart, J. J. P. *J. Comput. Chem.* **1989**, *10*, 221.

(25) VAMP calculations used version 5.6 (on an IBM RS-6000). See: Rauhut, G.; Chandrasekhar, J.; Alex, A.; Steinke, T.; Clark, T. *VAMP 5.0*, Oxford Molecular: Oxford, 1994.